
Supporting Information

Construction of a High-Efficiency Drug and Gene Co-Delivery System for Cancer Therapy from a pH-Sensitive Supramolecular Inclusion between Oligoethylenimine-graft- β -cyclodextrin and Hyperbranched Polyglycerol Derivative

Xiaoyan Zhou ^{1,2}, Lanqin Xu ³, Jiake Xu ⁴, Jianping Wu ⁵, Thomas Brett Kirk ⁵, Dong Ma ^{1,*}, Wei Xue ^{1,6,7,*}

¹ Key Laboratory of Biomaterials of Guangdong Higher Education Institutes, Guangdong Provincial Engineering and Technological Research Center for Drug Carrier Development, Department of Biomedical Engineering, Jinan University, Guangzhou 510632, China

² National Engineering Research Center for Healthcare Devices, Guangdong Key Lab of Medical Electronic Instruments and Polymer Material Products, Guangdong Institute of Medical Instruments, Guangzhou 510500, China

³ School of Pharmaceutical Sciences, Guangzhou Medical University, Guangzhou 511436, China

⁴ The School of Pathology and Laboratory Medicine, University of Western Australia, Perth 6009, Australia

⁵ 3D Imaging and Bioengineering Laboratory, Department of Mechanical Engineering, Curtin University, Perth 6845, Australia

⁶ Institute of Life and Health Engineering, Key Laboratory of Functional Protein Research of Guangdong Higher Education Institutes, Jinan University, Guangzhou 510632, China

⁷ The First Affiliated Hospital of Jinan University, Guangzhou 510630, China

E-mail addresses: tmadong@jnu.edu.cn (Dong Ma), weixue_jnu@aliyun.com (Wei Xue)

1. Characterization of PCL-HPG-BM and β -CD-PEI600

The chemical structure of PCL-HPG-BM was confirmed by ^1H NMR (Fig. S1). The peaks located at 1.3, 1.6 and 2.3 ppm were assigned to the protons of methylene groups in the 4-arms-PCL main chains. The signal at 3.99 ppm corresponding to the terminal methylene protons of 4-arms-PCL can also be identified. The peaks at 3.4 and 4.6 ppm were ascribed to the protons of the methylene/methenyl and hydroxy of HPG segments respectively. Besides, the peaks ranging from 7.50 to 8.50 ppm belonged to the protons of BM.

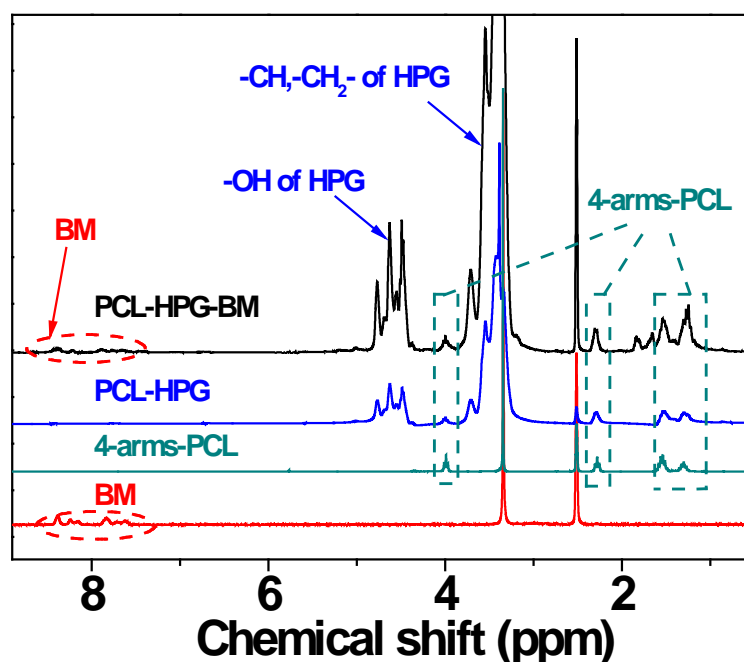


Fig. S1. ^1H NMR spectra of PCL-HPG-BM, PCL-HPG, 4-arms-PCL and BM.

Fig. S2 shows the ^1H NMR spectra of β -CD-PEI600 polymer in comparison with the starting β -CD and PEI600. The typical signals from H-1 of β -CD and PEI600 ethylene protons appeared at 5.0 and 2.5-3.0 ppm, respectively. Meanwhile, the number of grafted β -CD was determined to be 1.5 for PEI600 according to the peak integrals of β -CD H-1 signals and PEI600 ethylene proton signals.

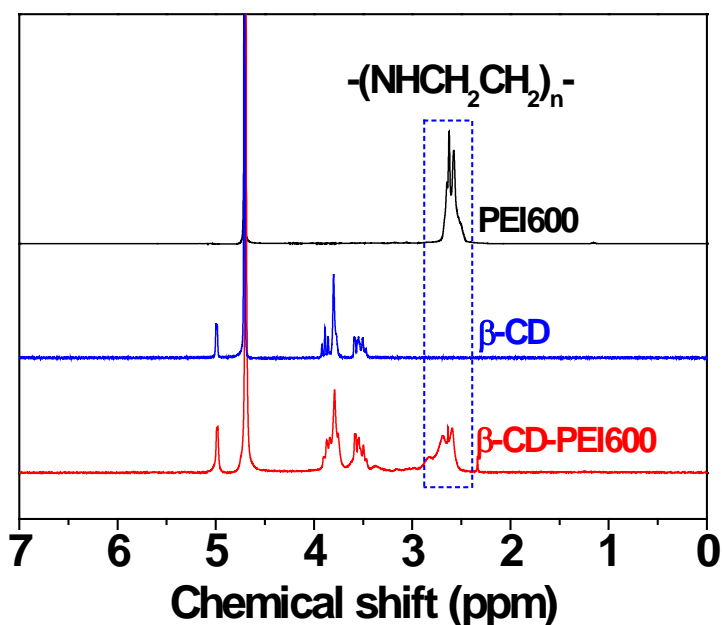


Fig. S2. ^1H NMR spectra of PEI600, β -CD and β -CD-PEI600.

2. Cellular uptake analyses of PCL-HPG-PEI600/DOX

Using the auto-fluorescence feature of DOX, the cellular uptake of the PCL-HPG-PEI600/DOX was measured by flow cytometry. Cellular uptake at different time (0.5, 2, 4 and 8 h) was performed as shown in Fig. S3. With the increasing incubation time, the red fluorescence intensity increased significantly, indicating that the uptake of PCL-HPG-PEI600/DOX complex was time-dependent. To detect the PCL-HPG-PEI600/DOX through which pathways to enter the cells, several specific pharmacological inhibitors were employed to block endocytosis pathways. As shown in Fig. S4, at 4°C , the uptake rate decreased significantly compared that of 37°C , indicating the endocytosis process was energy dependent. Besides, the red fluorescence intensity of cells pretreated with genistein, wortmannin and cytochalasin B did not exhibit a significant change, demonstrating treatments with genistein, wortmannin and cytochalasin B do not interfere with the endocytosis process. However, the uptake of PCL-HPG-PEI600/DOX was obviously inhibited by chlorpromazine, suggesting that clathrin-dependent endocytosis was the main endocytosis pathway of PCL-HPG-PEI600/DOX into MCF-7 cells.

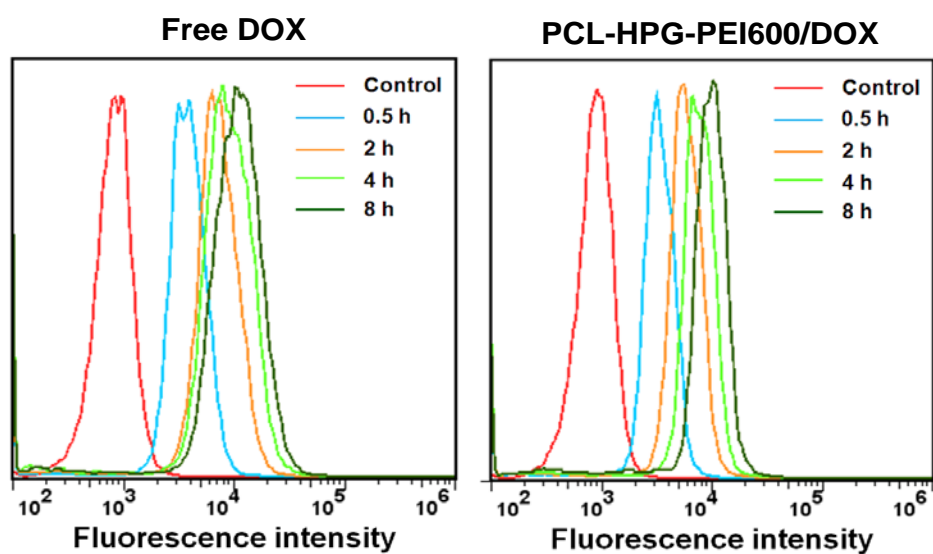


Fig. S3. Flow cytometry analysis of DOX in MCF-7 cells incubated with free DOX or PCL-HPG-PEI600/DOX for different time. The equivalent dose of DOX was 5 $\mu\text{g}/\text{mL}$.

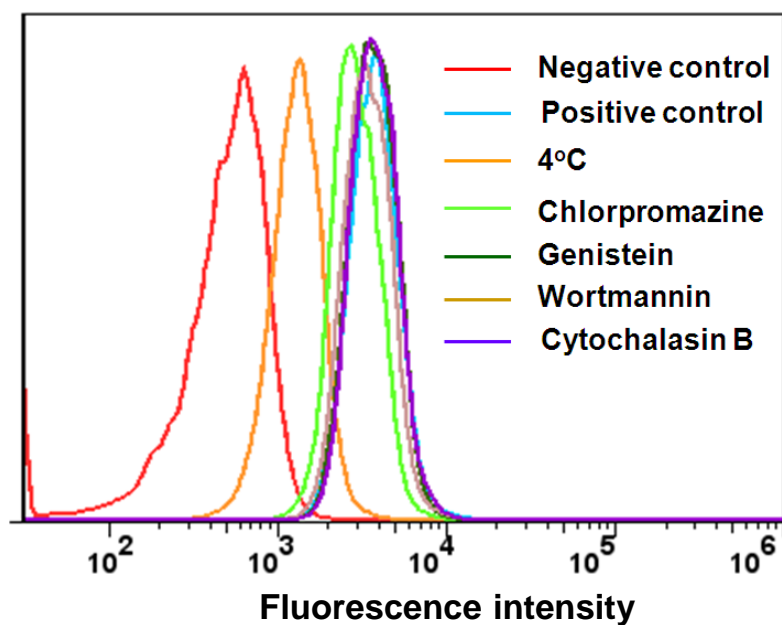


Fig. S4. Flow cytometry analysis of the effect of various inhibitors on the endocytosis of PCL-HPG-PEI600/DOX into MCF-7 cells.

3. Transfection efficiency and biocompatibility of PCL-HPG-PEIs

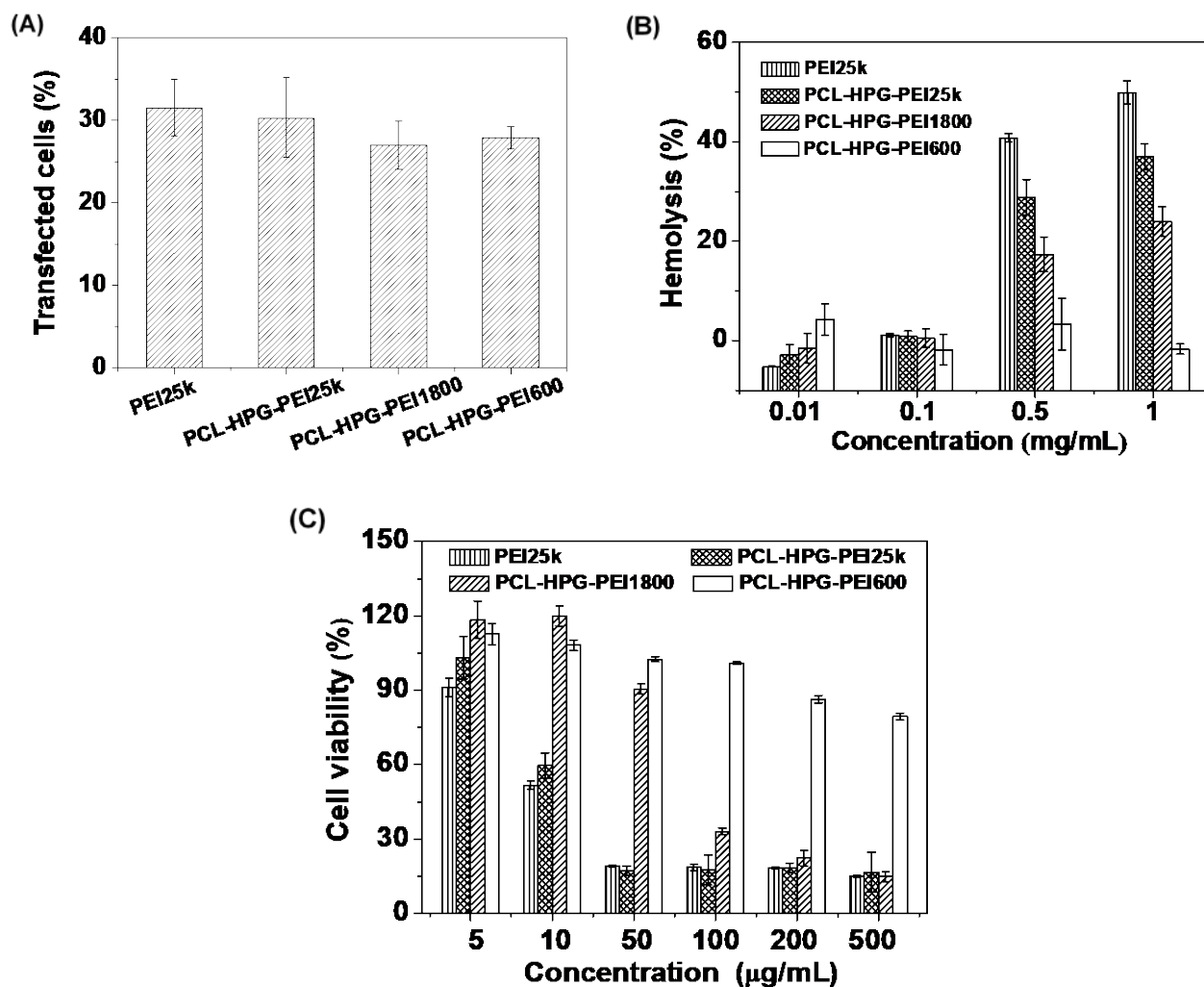


Fig. S5. The optimum transfection efficiency (A), hemolysis effect (B) and cytotoxicity (C) of PEI25k, PCL-HPG-PEI25k, PCL-HPG-PEI1800 and PCL-HPG-PEI600.

In our previous study, the optimum gene transfection efficiency of PCL-HPG-PEIs (using different molecular weight of PEI) in the absence of serum in MCF-7 cells was investigated. PEI25k was used as the control group. Fig. S5A shows the transfection results, there was no significant difference in transfection efficiency among PCL-HPG-PEI25k, PCL-HPG-PEI1800 and PCL-HPG-PEI600, indicating the low-molecular-weight PEI performed the excellent gene delivery ability after the supramolecular construction. It is important to note that the molecular weight of PEI is still an important factor affecting the transfection efficiency. The optimal transfection quality ratio of different PCL-HPG-PEIs is different. The optimum transfection quality ratio of

PCL-HPG-PEI25k、PCL-HPG-PEI1800 and PCL-HPG-PEI600 is 3:1, 50:1 and 120:1, respectively. In addition, to evaluate the biocompatibility of PCL-HPG-PEIs, the hemolysis assay and the cytotoxicity assay of the blank PCL-HPG-PEIs were performed. As shown in Fig. S5B, PCL-HPG-PEI600 did not cause any hemolysis even its concentration up to 1 mg/mL, the hemolytic ratio was lower than 5%. On the contrary, the obvious hemolysis was observed when the PEI25k, PCL-HPG-PEI25k and PCL-HPG-PEI1800 were used even if its concentration was only 0.5 mg/mL. Moreover, as presented in Fig. S5C, the PCL-HPG-PEI600 was not shown to exhibit significant toxicity to the MCF-7 cells even its concentration reached to 500 μ g/mL. However, the PEI25k, PCL-HPG-PEI25k and PCL-HPG-PEI1800 showed serious cytotoxicity. This result suggested that after the supramolecular construction, the supramolecular inclusion performed the excellent gene delivery ability as the high-molecular-weight PEI, and the excellent biocompatibility as the low-molecular-weight PEI.

4. The stability assay

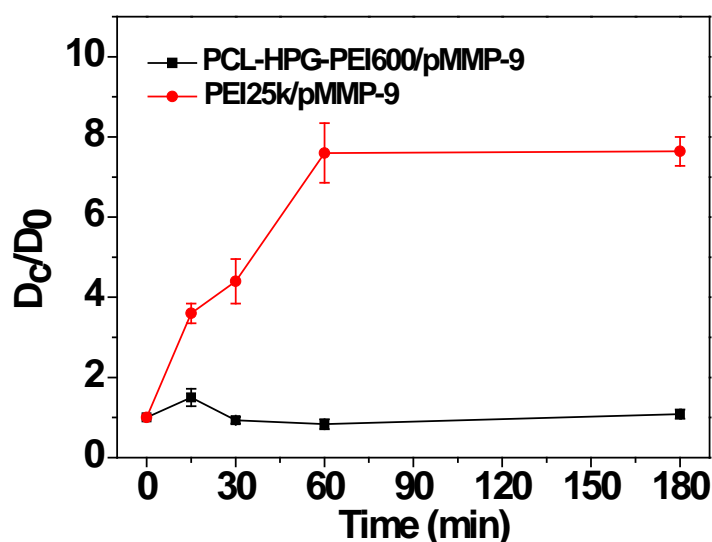


Fig. S6. The changes of the complexes size in 10% serum medium. (D_c denotes the complexes size at the certain time, D_0 denotes the complexes size at the start of the experiment.)

One of the significant challenges in the application of polycation/DNA complexes is physiological stability. The stability of the PCL-HPG-PEI600/pMMP-9 complexes and PEI25k/pMMP-9 complexes was evaluated by DLS in 10% serum medium. As shown in Fig. S6.

The stability assay showed that the PCL-HPG-PEI600/pMMP-9 complexes remained stable with a slight size change but no aggregation appeared. However, the particle size of the PEI25k/pMMP-9 complexes increased greatly. This result further indicates that the PCL-HPG-PEI600/pMMP-9 complex has better stability than the PEI25k/pMMP-9 complexes in the presence of serum.

5. Cellular uptake analyses of PCL-HPG-PEI600/gene complexes

The cellular uptake of the PCL-HPG-PEI600/gene complexes was also measured by flow cytometry. Cellular uptake at different time (0.5, 2, 4 and 8 h) was performed as shown in Fig. S7. With the increasing incubation time, the green fluorescence intensity of PCL-HPG-PEI600/siRNA increased significantly. However, the fluorescence intensity of PEI25k/siRNA showed no remarkable increase in 4 h. The results indicated that the PCL-HPG-PEI600/siRNA displayed the excellent blood stability and could be uptaken efficiently by MCF-7 cells. To detect the PCL-HPG-PEI600/gene complexes through which pathways to enter the cells, several specific pharmacological inhibitors were employed to block endocytosis pathways. As shown in Fig. S8, the green fluorescence intensity of cells pretreated with chlorpromazine exhibited a significant decrease, suggesting that clathrin-dependent endocytosis was the main endocytosis pathway of PCL-HPG-PEI600/gene complexes into MCF-7 cells.

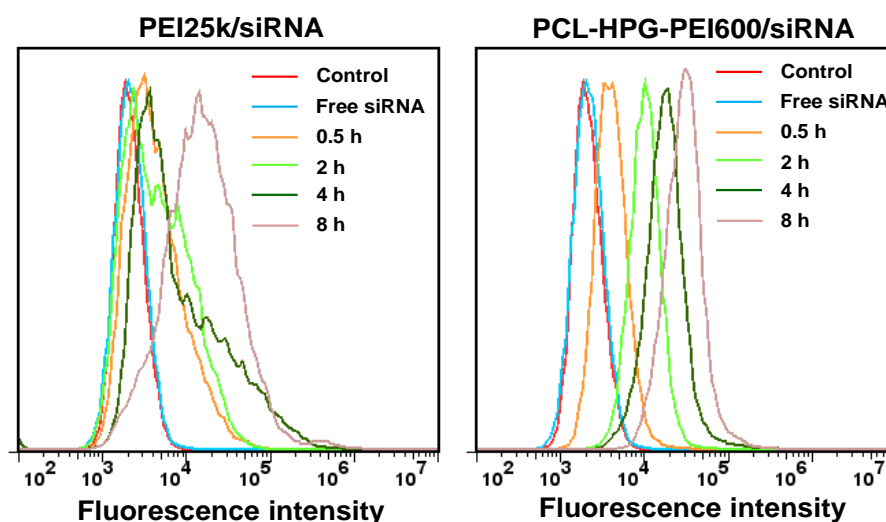


Fig. S7. Flow cytometry analysis of siRNA-FAM in MCF-7 cells incubated with PEI25k/siRNA or PCL-HPG-PEI600/siRNA for different time.

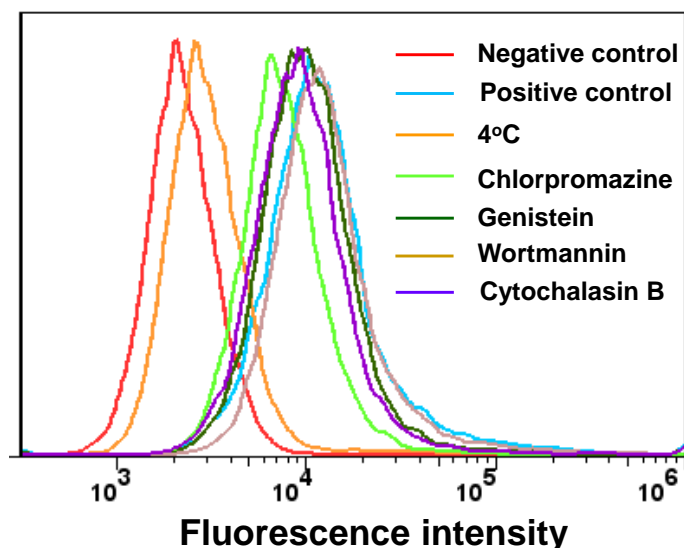


Fig. S8. Flow cytometry analysis of the effect of various inhibitors on the endocytosis of PCL-HPG-PEI600/siRNA into MCF-7 cells.

6. The endocytosis pathway of the co-delivery system

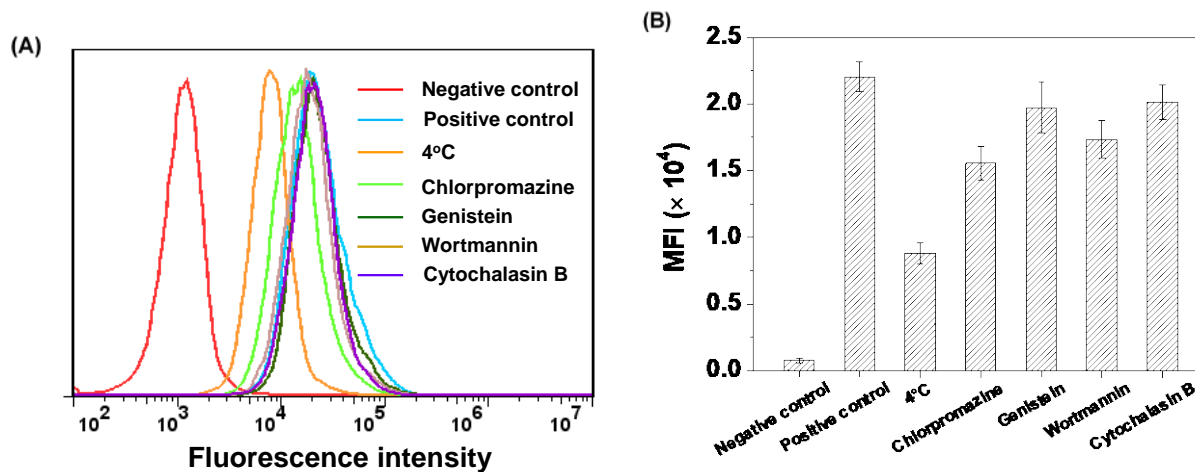


Fig. S9. Flow cytometry analysis (A) and quantification (B) of the effect of various inhibitors on the endocytosis of PCL-HPG-PEI600/DOX/pMMP-9 into MCF-7 cells.

To detect the PCL-HPG-PEI600/DOX/pMMP-9 complexes through which pathway to enter the cells, several specific pharmacological inhibitors were employed to block endocytosis pathways and the red fluorescence intensity of DOX were measured by flow cytometry. Consistent with the

endocytosis pathway analyses of PCL-HPG-PEI600/DOX and PCL-HPG-PEI600/gene complexes, as shown in Fig. S9, at 4°C, the uptake rate decreased significantly compared that of 37°C. In addition, the red fluorescence intensity of cells pretreated with chlorpromazine also exhibited obviously decreased, suggesting that clathrin-dependent endocytosis was still the main endocytosis pathway of PCL-HPG-PEI600/DOX/pMMP-9 into MCF-7 cells.

7. Transwell assay

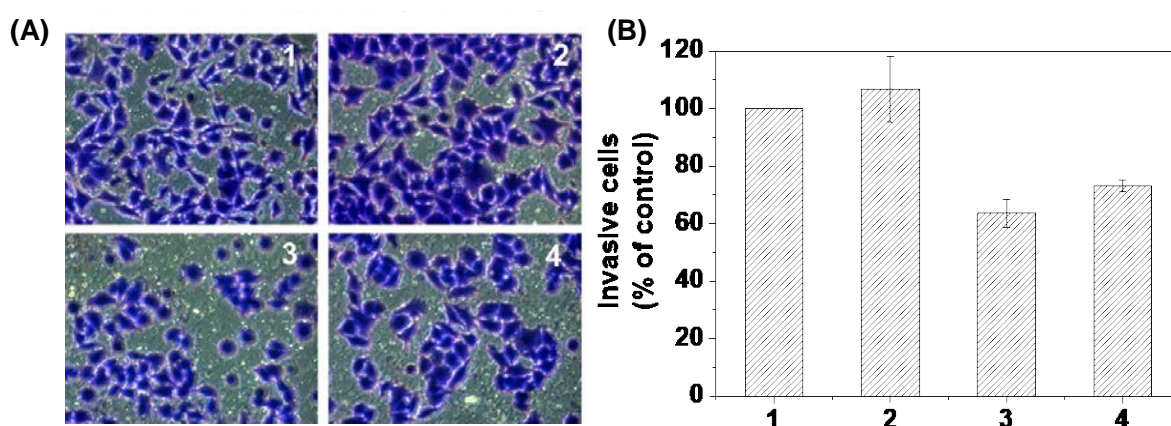


Fig. S10. (A, B) Inhibition and the relative quantitative results of cell invasion/migration after treatment with different formulations in MCF-7 cells. (1:PBS control; 2: blank PCL-HPG-PEI600; 3: PCL-HPG-PEI600/pMMP-9; 4: PEI25k/pMMP-9).

Cellular migration could promote the neovascularization, which is an important factor for tumor growth and metastasis and then compromises the therapeutic efficacy. The inhibition effect on MCF-7 cells migration of the different formulations (PCL-HPG-PEI600/pMMP-9 and PEI25k/pMMP-9) was performed by transwell assays. As shown in Fig. S10A and B, the blank PCL-HPG-PEI600 showed no significant difference with PBS control in cell invasion ratios, while both PCL-HPG-PEI600/pMMP-9 and PEI25k/pMMP-9 could reduce MCF-7 cells invasion ratios significantly. Particularly, for the PCL-HPG-PEI600/pMMP-9, the number of MCF-7 cells invaded through transwell, which was lower than that of PEI25k/pMMP-9. The results further confirmed PCL-HPG-PEI600/pMMP-9 complexes was more effective in decreasing the MCF-7 cell migration than that of PEI25k/pMMP-9 complexes.

8. Cytotoxicity

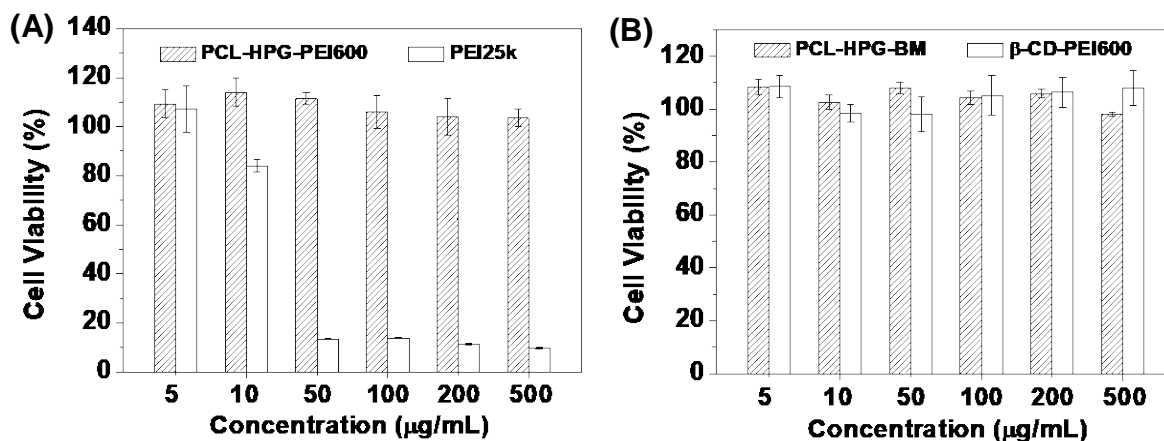


Fig. S11. (A) CCK-8 results of PCL-HPG-PEI600 and PEI25k at different concentrations on 3T3 cells. (B) CCK-8 results of PCL-HPG-BM and β -CD-PEI600 at different concentrations on 3T3 cells.

As a good carrier, low cytotoxicity of vector itself was essential for practical applications. Therefore, CCK-8 assay was carried out to investigate the cytotoxicity of the blank PCL-HPG-PEI600 in 3T3 cells. PEI25k was used as a control. As presented in Fig. S11A, as expected, the blank PCL-HPG-PEI600 was not shown to exhibit significant toxicity to the 3T3 cells even its concentration up to 500 $\mu\text{g/mL}$, the cell viability was still about 100%. However, the PEI25k showed serious cytotoxicity and no more than 20% cells were viable after treated with 50 $\mu\text{g/mL}$ PEI25k. Additionally, the cytotoxicity of degradation products (PCL-HPG-BM and β -CD-PEI600) to 3T3 cells also has been studied, the results as shown in Fig S11B, PCL-HPG-BM and β -CD-PEI600 showed no significant toxicity to 3T3 cells at concentrations below 500 $\mu\text{g/mL}$.